AD-A124 282 THE EFFECT OF RANDOM STEERING VECTOR ERRORS IN THE 1/1
APPLEBAUM ADAPTIVE ARRAY(U) OHIO STATE UNIV COLUMBUS
ELECTROSCIENCE LAB R T COMPTON JUN 82 ESL-713603-7
UNCLASSIFIED N00019-81-C-0093 F/G 9/5 NL

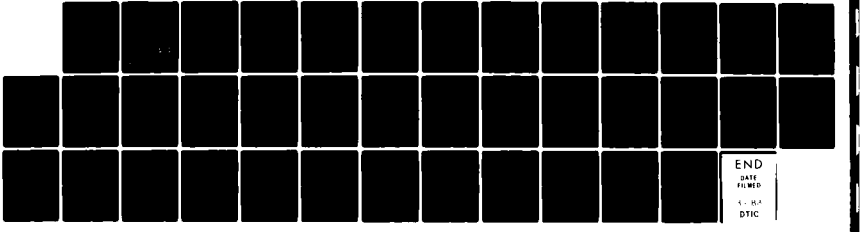

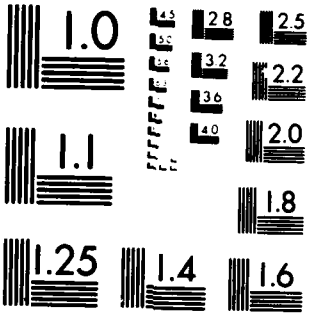

(11)

OSU

The Ohio State University

THE EFFECT OF RANDOM STEERING VECTOR ERRORS IN THE APPLEBAUM ADAPTIVE ARRAY

R.T. Compton, Jr.

The Ohio State University

ElectroScience Laboratory

Department of Electrical Engineering
Columbus, Ohio 43212

Technical Report 713603-7

Contract Number N00019-81-C-0093

June, 1982

Naval Air Systems Command
Washington, D.C. 20361

NOTICES

When Government drawings, specifications, or other data are used for any purpose other than in connection with a definitely related Government procurement operation, the United States Government thereby incurs no responsibility nor any obligation whatsoever, and the fact that the Government may have formulated, furnished, or in any way supplied the said drawings, specifications, or other data, is not to be regarded by implication or otherwise as in any manner licensing the holder or any other person or corporation, or conveying any rights or permission to manufacture, use, or sell any patented invention that may in any way be related thereto.

50272-101

REPORT DOCUMENTATION PAGE	1. REPORT NO.	2. AD-A104282	3. Recipient's Accession No

4. Title and Subtitle

THE EFFECT OF RANDOM STEERING VECTOR ERRORS IN THE APPLEBAUM ADAPTIVE ARRAY

5. Report Date

6.

7. Author(s)
R.T. Compton, Jr.

8. Performing Organization Rept. No
713603-7

9. Performing Organization Name and Address
The Ohio State University ElectroScience Laboratory
Department of Electrical Engineering
Columbus, Ohio 43212

10. Project/Task/Work Unit No.

11. Contract(C) or Grant(G) No
(C) N00019-81-C-0093
(G)

12. Sponsoring Organization Name and Address
Naval Air Systems Command
Washington, D.C. 20361

13. Type of Report & Period Covered
Technical

14.

15. Supplementary Notes

16. Abstract (Limit: 200 words)

This report examines the effect of random errors in the steering vector of an Applebaum adaptive array. Each component of the steering vector is assumed to have a random error component uncorrelated between elements. The array output signal-to-interference-plus-noise ratio (SINR) is computed as a function of the error variance.

It is shown that the array output SINR becomes more sensitive to steering vector errors as more elements are added to the array and as the received desired signal power becomes larger. The variance of the steering vector error that may be tolerated depends on the required desired signal dynamic range. The larger the dynamic range that must be accomodated, the smaller the error variance must be.

17. Document Analysis a. Descriptors

b. Identifiers/Open-Ended Terms

c. COSATI Field/Group

18. Availability Statement	19. Security Class (This Report)	21. No. of Pages
	Unclassified	32
	20. Security Class (This Page)	22. Price
	Unclassified	

(See ANSI-Z39.18) See Instructions on Reverse OPTIONAL FORM 272 (4-77) (Formerly NTIS-35) Department of Commerce

TABLE OF CONTENTS

		Page
LIST OF FIGURES		iv
I.	INTRODUCTION	1
II.	FORMULATION	3
III.	RESULTS	15
IV.	CONCLUSIONS	31
REFERENCES		32

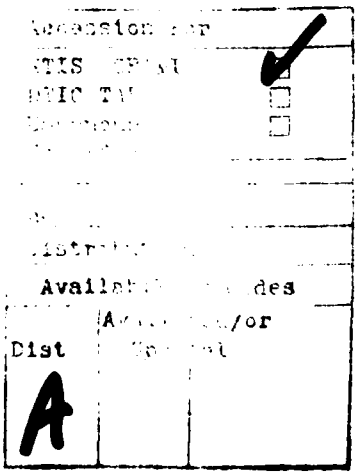

LIST OF FIGURES

Figure		Page
1	An N-element adaptive array.	5
2	SINR vs σ_w^2 No interference, $\theta_d = 0°$, $B_d = 0$, SNR = 0 dB.	16
3	SINR vs σ_w^2 No interference, $\theta_d = 0°$, $B_d = 0$, SNR = 10 dB.	17
4	SINR vs σ_w^2 No interference, $\theta_d = 0°$, $B_d = 0$, SNR = 20 dB.	18
5	SINR vs σ_w^2 No interference, 3 elements, $\theta_d = 0°$, $B_d = 0$.	19
6	SINR vs σ_w^2 $\theta_d = 0°$, $B_d = 0$, SNR = 0 dB $\theta_i = 30°$, $B_i = 0$, INR = 40 dB .	20
7	SINR vs σ_w^2 $\theta_d = 0°$, $B_d = 0$, SNR = 10 dB $\theta_i = 30°$, $B_i = 0$, INR = 40 dB .	21
8	SINR vs σ_w^2 $\theta_d = 0°$, $B_d = 0$, SNR = 20 dB $\theta_i = 30°$, $B_i = 0$, INR = 40 dB .	22
9	SINR vs σ_w^2 3 elements, $\theta_d = 0°$, $B_d = 0$ $\theta_i = 30°$, $B_i = 0$, INR = 40 dB .	23

Figure		Page
10	SINR vs SINR No interference, 3 elements $\theta_d = 0°$, $0 \leq B_d \leq 0.5$.	26
11	SINR vs SINR No interference, 3 elements $\theta_d = 90°$, $\sigma_w^2 = 0$.	28
12	SINR vs SINR No interference, 3 elements $\theta_d = 90°$.	29
13	SINR vs SINR 3 elements, $\theta_d = 0°$, $0 \leq B_d \leq 0.1$ $\theta_i = 30°$, INR = 40 dB.	30

I. INTRODUCTION

Applebaum's original adaptive array concept [1] uses a steering vector in the weight control loops. This steering vector controls the quiescent pattern of the array and can be used to point a beam in the direction of the desired signal. Our purpose in this paper is to discuss the effect of random errors in this steering vector.

When the Applebaum array is used in radar, the desired signal is often a weak pulsed signal with a pulse width that is very short compared to the time constants of the array feedback loops. In this case the array pattern is not affected much by the desired signal, because the desired signal is not present long enough to have much impact on the weights. The array does not null the desired signal, and minor errors in the steering vector are of little consequence.

In communication applications of these arrays, however, the desired signal may be present continuously and may also be a strong signal. In this case the array is much more sensitive to errors in the steering vector, because the array may null the desired signal. With a continuous desired signal present, the array feedback attempts to minimize the array output desired signal power. If the steering vector components are properly set, and the desired signal is strong, the array does this by simply lowering the absolute magnitude of the array pattern. Lowering the pattern magnitude reduces the array output desired signal power, interference power and thermal noise power all proportionately, so the output signal-to-interference-plus-noise ratio (SINR) is not affected. But if the steering vector is incorrectly

set, the array feedback will null the desired signal without reducing the output thermal noise or interference power. The result is a rapid drop in output SINR. For this reason, the performance of the array is sensitive to steering vector errors.

In a previous paper [2], the author described the effect on array performance of one type of steering vector error, a beam pointing error. A beam pointing error occurs when the actual desired signal arrival angle is different from its assumed or estimated value. In that paper, the steering vector components were correct except that they were chosen for a beam in a slightly different direction from the desired signal.

In the present paper, we study the effects of random errors in the steering vector components. We assume the steering vector has been chosen to produce a beam in the proper direction, but that each component of the steering vector has a random error, uncorrelated from one element to another. We show how the output SINR depends on the variance of the steering vector errors. We include in our model the effects of signal powers, arrival angles and bandwidths, and also the number of elements in the array. The results show how accurate a steering vector has to be for a given level of array performance.

In practice, random steering vector errors can occur for different reasons, depending on how the steering vector is derived. For example, one way to determine a steering vector is to allow an LMS array (using a reference signal [3,4]) to adapt to a desired signal during an interval

where it is known that there is no interference. The weights obtained during this interval may then be used as steering weights during a later interval when interference may be present. However, steering vector components obtained in this way will have random errors because of the noise present in the array feedback loops when the weights are measured. Another way of obtaining a steering vector is to compute it, based on a known signal arrival angle. However, the steering vector computed may differ from its ideal value because receiver sensitivities, antenna gains, etc., in the actual array differ from the values assumed in the computation. Moreover, even a correctly computed steering vector can be carried to only so many places of accuracy, because of truncation, either in the calculations or in the storage of the steering vector. The difference between the computed steering vector and the ideal one is an error that must be kept small. The accuracy required can be determined from the curves given here.

Section II of the paper defines the problem, establishes notation and develops the necessary equations. Section III contains the results.

II. FORMULATION

Consider the N-element adaptive array shown in Figure 1. The elements are assumed to be isotropic and to lie in a straight line with half wavelength spacing. $\tilde{x}_j(t)$ is the analytic signal received on element j. $\tilde{x}_j(t)$ is multiplied by complex weight w_j and summed to produce the array output $\tilde{s}(t)$. We assume the weights are controlled by Applebaum correlation loops [1], or by computer control [5], such that the steady-state weight vector $W = (w_1, w_2, \ldots, w_N)^T$ is given by

$$W = \Phi^{-1} W_S \ , \qquad (1)$$

where Φ is the covariance matrix

$$\Phi = E(X^* X^T) \tag{2}$$

and W_s is the steering vector

$$W_s = (w_{s1}, w_{s2}, \ldots, w_{sN})^T. \tag{3}$$

In these equations T denotes transpose, * complex conjugate and E(.) expectation. X is the signal vector

$$X = (\tilde{x}_1(t), \tilde{x}_2(t), \ldots, \tilde{x}_N(t))^T. \tag{4}$$

In this paper we are interested in how random errors in the steering vector W_s affect the performance of the array. To have a specfic problem to study, we shall suppose a desired signal and one interference signal are incident on the array. Also, we assume each element signal $\tilde{x}_j(t)$ contains thermal noise as well. Thus, the j^{th} element signal has the form

$$\tilde{x}_j(t) = \tilde{d}_j(t) + \tilde{i}_j(t) + \tilde{n}_j(t), \tag{5}$$

where $\tilde{d}_j(t)$ is the desired signal, $\tilde{i}_j(t)$ is the interference and $\tilde{n}_j(t)$ is the thermal noise. These signals are defined as follows.

Let the desired signal arrive from angle θ_d relative to broadside. (θ is defined in Figure 1.) The desired signal in each element is then a delayed version of that in element 1,

$$\tilde{d}_j(t) = \tilde{d}\left[t-(j-i)\,\tau_d\right], \tag{6}$$

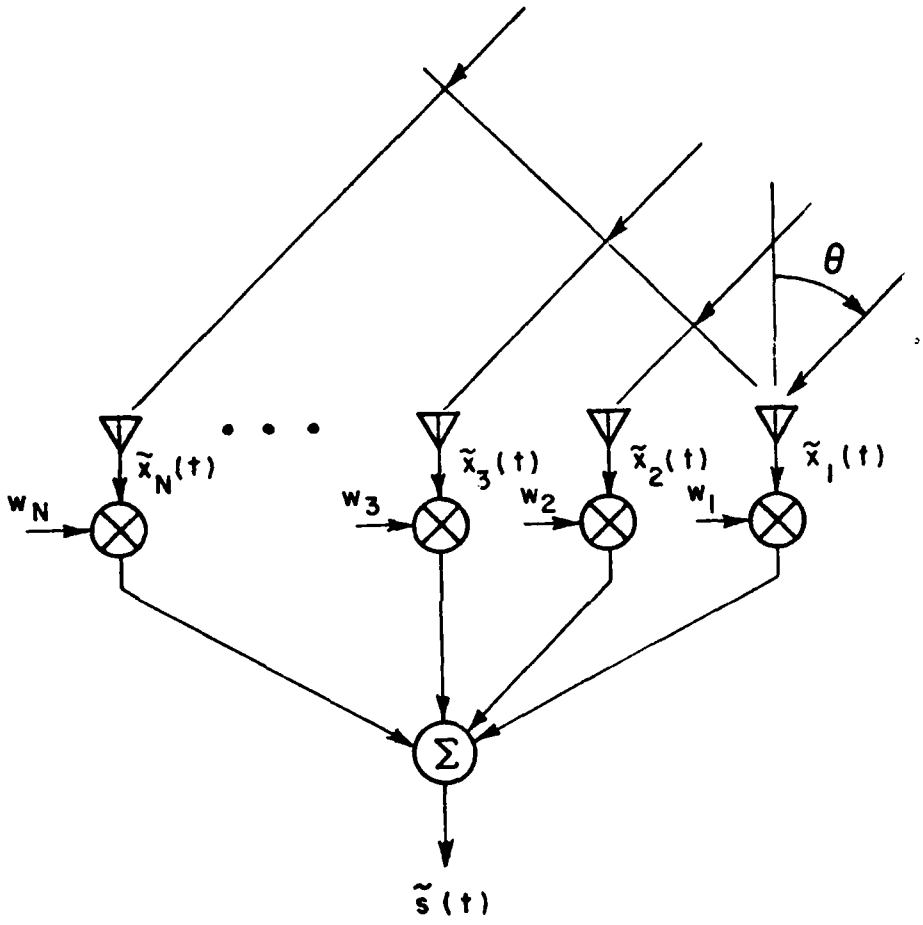

Figure 1. An N-element adaptive array.

where $\tilde{d}(t)$ is the desired signal waveform on element 1 and T_d is the time delay between two adjacent elements in the array,

$$T_d = \frac{\ell}{c} \sin \theta_d, \tag{7}$$

with ℓ the element separation and c the velocity of propagation.

Similarly, let the interference arrive from angle θ_i, so

$$\tilde{i}_j(t) = \tilde{i}\left[t - (j - 1)\, T_i \right], \tag{8}$$

where

$$T_i = \frac{\ell}{c} \sin \theta_i, \tag{9}$$

with $\tilde{i}(t)$ the interference waveform on element 1.

Finally, let the thermal noise components $\tilde{n}_j(t)$ be independent, zero mean, bandlimited Gaussian noise signals with variance σ^2,

$$E\left[\tilde{n}_j^{*}(t)\, \tilde{n}_k(t)\right] = \sigma^2 \delta_{jk}, \tag{10}$$

where δ_{jk} is the Kronecker delta. The signals $\tilde{d}(t)$, $\tilde{i}(t)$ and $\tilde{n}_j(t)$ are all assumed statistically independent of each other.

Because of (5), the signal vector X in (4) may also be split into its desired, interference and noise components:

$$X = X_d + X_i + X_n. \tag{11}$$

Then because X_d, X_i and X_n are statistically independent, the covariance matrix in (2) may be written

$$\Phi = \Phi_d + \Phi_i + \Phi_n, \tag{12}$$

where Φ_d is the covariance matrix for the desired signal,

$$\Phi_d = E(X_d^* X_d^T) = \begin{pmatrix} R_d(o) & R_d(-T_d) & \cdots & R_d[-(N-1)T_d] \\ R_d(T_d) & R_d(o) & & \cdot \\ \cdot & \cdot & \cdot & \cdot \\ \cdot & \cdot & \cdot & \cdot \\ \cdot & \cdot & \cdot & \cdot \\ R_d[(N-1)T_d] & \cdot & \cdot & R_d(o) \end{pmatrix} \tag{13}$$

Φ_i is the covariance matrix for the interference,

$$\Phi_i = E(X_i^* X_i^T) = \begin{pmatrix} R_i(o) & R_i(-T_i) & \cdots & R_i[-(N-1)T_i] \\ R_i(T_i) & R_i(o) & & \\ \cdot & \cdot & \cdot & \cdot \\ \cdot & \cdot & \cdot & \cdot \\ \cdot & \cdot & \cdot & \cdot \\ R_i[(N-1)\ T_i] & \cdot & \cdot & R_i(o) \end{pmatrix} \tag{14}$$

and Φ_n is the covariance matrix for the thermal noise,

$$\Phi_n = E(X_n^*\ X_n^T) = \sigma^2 I. \tag{15}$$

In these equations I is the identity matrix and $R_d(\tau)$ and $R_i(\tau)$ are the autocorrelation functions of $\tilde{d}(t)$ and $\tilde{i}(t)$:

$$R_d(\tau) = E\left[\tilde{d}(t+\tau)\,\tilde{d}^*(t)\right] , \tag{16}$$

and

$$R_i(\tau) = E\left[\tilde{i}(t+\tau)\,\tilde{i}^*(t)\right] . \tag{17}$$

Since $R(-\tau) = R^*(\tau)$, Φ_d, Φ_i and Φ_n are Hermitian matrices.

To simplify our results later, it is helpful if we normalize these matrices. To do this, we define the signal powers,

$$S_d = R_d(o) = \text{desired signal power per element}, \tag{18}$$

and

$$S_i = R_i(o) = \text{interference power per element}, \tag{19}$$

the normalized autocorrelation functions,

$$\rho_d(\tau) = R_d(\tau)/S_d, \tag{20}$$

and

$$\rho_i(\tau) = R_i(\tau)/S_i, \tag{21}$$

and the signal-to-noise ratios

$$\xi_d = \frac{S_d}{\sigma^2} = \text{desired signal-to-noise ratio (SNR) per element}, \tag{22}$$

and

$$\xi_i = \frac{S_i}{\sigma^2} = \text{interference-to-noise ratio (INR) per element} \qquad (23)$$

With these definitions, the covariance matrices may be written

$$\Phi = \sigma^2 \Phi_o = \sigma^2(\Phi_{do} + \Phi_{io} + \Phi_{no}), \qquad (24)$$

where Φ_{do} is the normalized desired signal covariance matrix

$$\Phi_{do} = \xi_d \begin{pmatrix} \rho_d(o) & \rho_d(-T_d) & \cdots & \rho_d\left[-(N-1)\,T_d\right] \\ \rho_d(T_d) & & & \\ \vdots & & & \vdots \\ \rho_d\left[(N-1)\,T_d\right] & \cdots & & \rho_d(o) \end{pmatrix}, \qquad (25)$$

Φ_{io} is the normalized interference covariance matrix

$$\Phi_{io} = \xi_i \begin{pmatrix} \rho_i(o) & \rho_i(-T_i) & \cdots & \rho_i\left[-(N-1)\,T_i\right] \\ \rho_i(T_i) & & & \\ \vdots & & & \vdots \\ \rho_i\left[(N-1)\,T_i\right] & \cdots & & \rho_i(o) \end{pmatrix}, \qquad (26)$$

and Φ_{no} is the normalized noise covariance matrix

$$\Phi_{no} = I. \tag{27}$$

In order to carry out a specific calculation below, we shall assume the desired and interference signals each have a flat, band-limited power spectral density centered at frequency ω_o. We assume the desired signal has bandwidth $\Delta\omega_d$, so its autocorrelation function is

$$R_d(\tau) = S_d \frac{\sin\left(\frac{\Delta\omega_d\tau}{2}\right)}{\left(\frac{\Delta\omega_d\tau}{2}\right)} e^{j\omega_o\tau}. \tag{28}$$

Substituting $\tau = nT_d$ *and noting that*

$$\frac{\Delta\omega_d nT_d}{2} = \frac{n}{2}\left(\frac{\Delta\omega_d}{\omega_o}\right)\left(\omega_o T_d\right) = \frac{n}{2} B_d \phi_d, \tag{29}$$

where B_d is the fractional bandwidth

$$B_d = \frac{\Delta\omega_d}{\omega_o}, \tag{30}$$

and ϕ_d is the carrier phase shift between adjacent array elements,

$$\phi_d = \omega_o T_d, \tag{31}$$

we have

$$\rho_d(nT_d) = \frac{\sin\left(\frac{n}{2} B_d \phi_d\right)}{\left(\frac{n}{2} B_d \phi_d\right)} e^{jn\phi_d} . \tag{32}$$

Similarly, we assume the interference has bandwidth $\Delta\omega_i$ and define the fractional bandwidth

$$B_i = \frac{\Delta\omega_i}{\omega_o} , \tag{33}$$

and phase shift

$$\phi_i = \omega_o T_i . \tag{34}$$

Then

$$\rho_i(nT_i) = \frac{\sin\left(\frac{n}{2} B_i \phi_i\right)}{\left(\frac{n}{2} B_i \phi_i\right)} e^{jn\phi_i} . \tag{35}$$

From (32) and (35), the covariance matrices in (24) - (26) can be found. The steady-state weight vector W in (1) is then given by

$$W = \Phi_o^{-1}\left(\frac{1}{\sigma^2} W_s\right) . \tag{36}$$

As stated above, our purpose in this paper is to investigate the effects of random errors in the steering vector W_s on the performance of the array. To this end, we write W_s in the form

$$W_S = W_1 + \Gamma_1 \quad , \tag{37}$$

where W_1 is the ideal steering vector and Γ_1 is an error vector. The ideal steering vector is the steering vector that maximizes the array response in the direction of the desired signal. Since the signal arrives from angle θ_d (and the elements are a half wavelength apart), we choose

$$W_1 = K_S W_O$$

$$= K_s\left(1, e^{j\pi\sin\theta_d}, e^{j2\pi\sin\theta_d}, \ldots e^{j(N-1)\pi\sin\theta_d} \right)^T \quad , \tag{38}$$

where K_S is an arbitrary constant. Γ_1 is a vector containing the steering vector errors. We write Γ_1 in the form

$$\Gamma_1 = K_S \Gamma = K_S \left(\gamma_1, \gamma_2, \ldots, \gamma_N\right)^T$$

$$= K_s(\gamma_{1r} + j\gamma_{1i}, \gamma_{2r} + j\gamma_{2i}, \ldots, \gamma_{Nr} + j\gamma_{Ni})^T \quad , \tag{39}$$

where K_S is the same constant as in (38). With W_O and Γ normalized in this way, each γ_k represents the error in the corresponding term $e^{j(k-1)\pi \sin \theta_d}$ of W_O. Since this term has unit magnitude, $|\gamma_k|$ may be regarded as the value of the error normalized to the magnitude of the ideal steering vector weight, i.e., the fractional error.

To evaluate the effects of random errors, we shall assume each real or imaginary component γ_{kr} or γ_{ki} of Γ is a statistically independent random variable with zero mean and variance σ_w^2, i.e.,

$$E\left[\gamma_{kP}\right] = 0, \tag{40}$$

and

$$E\left[\gamma_{kP}\gamma_{\ell Q}\right] = \sigma_w^2\ \delta_{k\ell}\ \delta_{PQ}\ , \tag{41}$$

where P and Q each stand for r (real) or i (imaginary).

When (37) - (39) are substituted in (36), the steady-state weight vector is

$$W = \frac{K_s}{\sigma^2}\ \Phi_o^{-1}\ (W_o + \Gamma). \tag{42}$$

For this weight vector, the desired signal component of the array output, $\tilde{s}_d(t)$, is

$$\tilde{s}_d(t) = X_d^T W, \tag{43}$$

so the output desired signal power P_d is

$$P_d = \frac{1}{2}\ E\ \{|\tilde{s}_d(t)|^2\} = \frac{1}{2}\ E\ \left\{ W^\dagger\ X_d^*\ X_d^T\ W \right\}$$

$$= \frac{K_s^2}{2\sigma^4}\ E\ \{(W_o^\dagger + \Gamma^\dagger)\ \ \Phi_o^{-1}\ X_d^*\ X_d^T\ \Phi_o^{-1}\ (W_o + \Gamma)\} \tag{44}$$

(where † denotes transpose conjugate). Here the expectation is taken over both the random components of Γ and over the signals in X_d. Averaging $X_d^*\ X_d^T$ gives

$$P_d = \frac{K_s^2}{2\sigma^2} \; E \{(W_o^\dagger + \Gamma^\dagger) \; \Phi_o^{-1} \; \Phi_{do} \; \Phi_o^{-1} \; (W_o + \Gamma) \} \; . \qquad (45)$$

When the expectation over Γ is carried out, the cross products between W_o and Γ average to zero, so we are left with

$$P_d = \frac{K_s^2}{2\sigma^2} \left[W_o^\dagger \Phi_o^{-1} \; \Phi_{do} \; \Phi_o^{-1} \; W_o + E \{\Gamma^\dagger \; \Phi_o^{-1} \; \Phi_{do} \; \Phi_o^{-1} \; \Gamma\} \right]$$

$$= \frac{K_s^2}{2\sigma^2} \left[W_o^\dagger \Phi_o^{-1} \; \Phi_{do} \; \Phi_o^{-1} \; W_o + 2\sigma_w^2 \; Tr\{\Phi_o^{-1} \; \Phi_{do} \; \Phi_o^{-1}\} \right] \; , \qquad (46)$$

where Tr (.) denotes the trace. A similar calculation of the output interference power P_i and output noise power P_n gives

$$P_i = \frac{K_s^2}{2\sigma^2} \left[W_o^\dagger \; \Phi_o^{-1} \; \Phi_{io} \Phi_o^{-1} \; W_o + 2\sigma_w^2 \; Tr \; \{\Phi_o^{-1} \; \Phi_{io} \; \Phi_o^{-1}\} \right] \; , \qquad (47)$$

and

$$P_n = \frac{K_s^2}{2\sigma^2} \left[\; W_o^\dagger \Phi_o^{-1} \; \Phi_o^{-1} \; W_o + 2\sigma_w^2 \; Tr \; \{\Phi_o^{-1} \; \Phi_o^{-1}\} \right] \; . \qquad (48)$$

We define the desired signal-to-interference-plus-noise ratio (SINR) out of the array to be

$$SINR = \frac{P_d}{P_i + P_n} \; . \qquad (49)$$

Note that the constant $K_s^2/2\sigma^2$ cancels out of this ratio and hence has no effect on the SINR.

In the next section we show curves of the SINR computed from (46)-(49) and discuss how the error variance σ_w^2 affects the array performance.

III. RESULTS

We begin by showing how the array output SINR depends on σ_w^2. Figures 2-9 show typical results computed for a number of cases.

First, Figures 2-4 show the output SINR as a function of σ_w^2 for the case where a desired signal arrives at broadside ($\theta_d = 0$) and for no interference. The three figures are for different SNR's. Figure 2 is for ξ_d = 0 dB, Figure 3 for ξ_d = 10 dB and Figure 4 for ξ_d = 20 dB. Each figure shows the SINR versus σ_w^2 for 2, 3, 4, 6, 8 and 10 elements in the array.

These figures show several interesting things. First, the array output SINR can drop rather rapidly with σ_w^2. For example, Figure 4 shows that when ξ_d = 20 dB and the array has 10 elements, the SINR drops from 30 dB for σ_w^2 = 0 to 10 dB for σ_w^2 = .0001. σ_w^2 = .0001 corresponds to an rms fractional error in each real and imaginary part of the steering vector of $\sqrt{.0001}$ = 1%.

Second, Figures 2-4 show that the sensitivity of the SINR to σ_w^2 increases with the number of elements in the array. The more elements, the faster the SINR drops with σ_w^2. Moreover, when σ_w^2 exceeds a certain value, increasing the number of elements in the array will actually <u>decrease</u> the output SINR. If ξ_d = 10 dB, for example, Figure 3 shows that for σ_w^2 = .001 the SINR is highest with 2 elements and drops as more elements are added. To be able to increase the SINR by adding

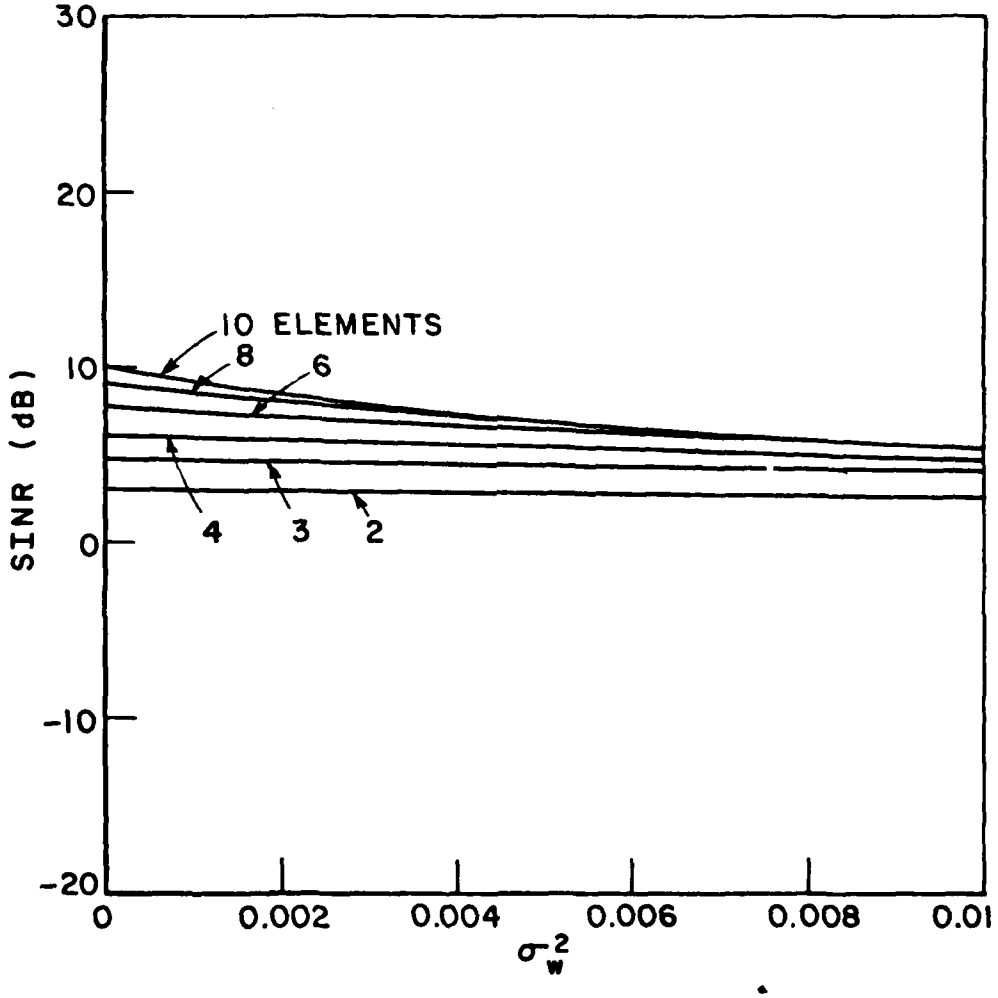

Figure 2. SINR vs σ_w^2

No interference, $\theta_d = 0^o$, $B_d = 0$, SNR = 0 dB

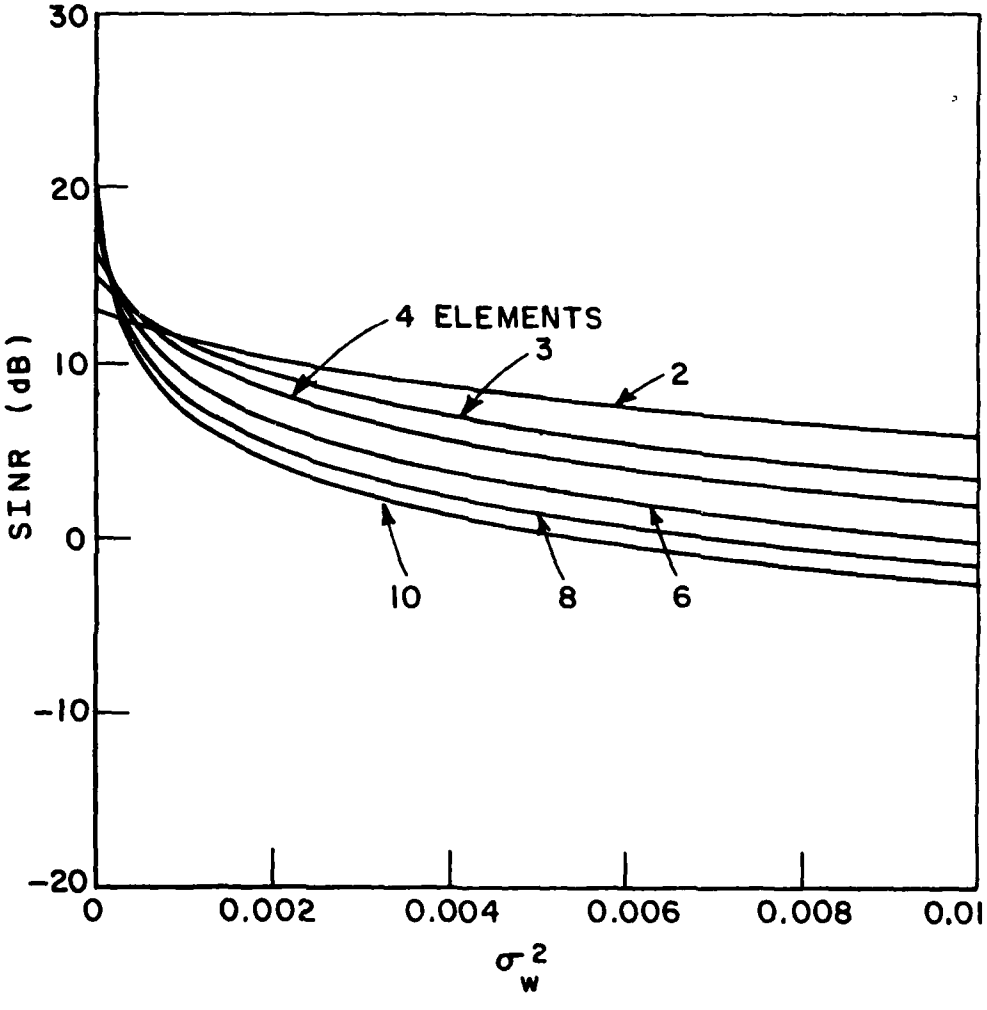

Figure 3. SINR vs σ_w^2

No interference, $\theta_d = 0^o$, $B_d = 0$, SNR = 10 dB

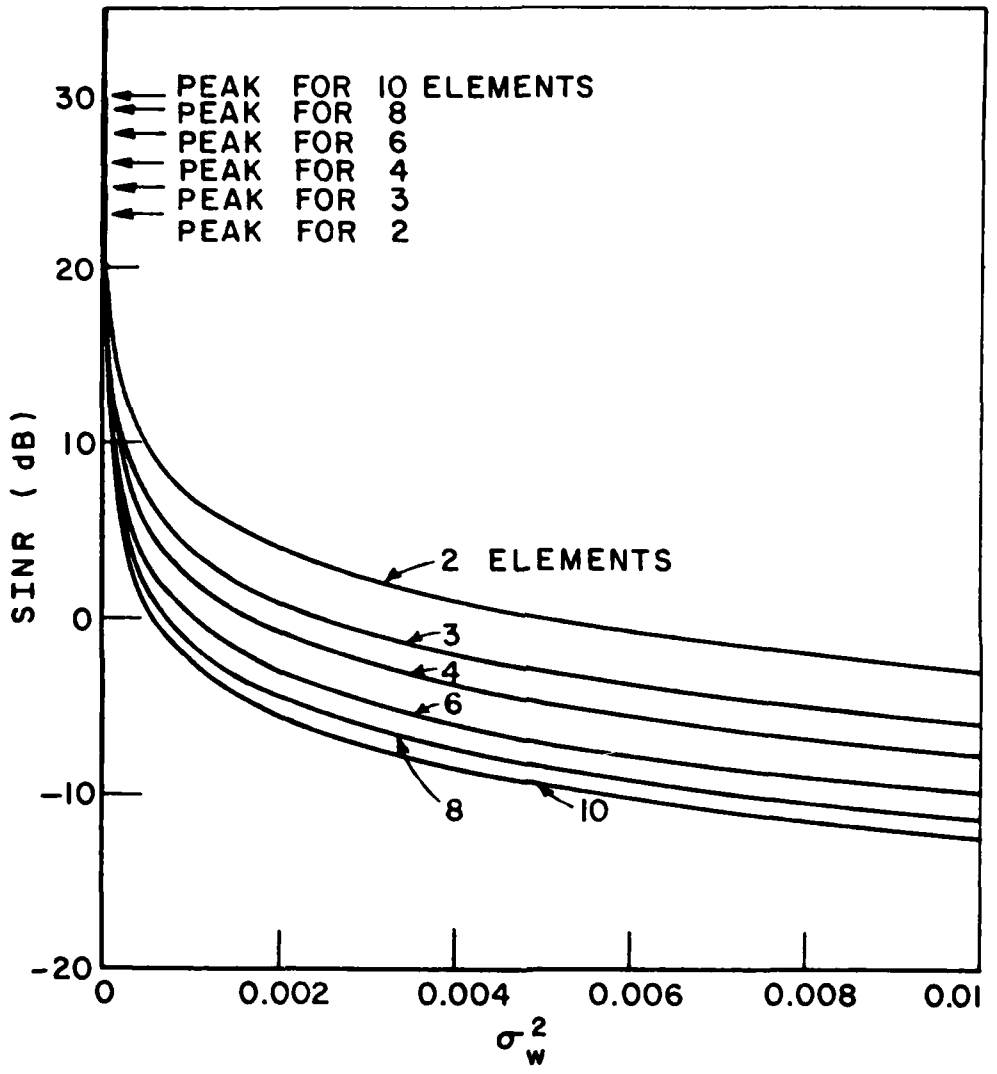

Figure 4. SINR vs σ_w^2

No interference, $\theta_d = 0^o$, $B_d = 0$, SNR = 20 dB

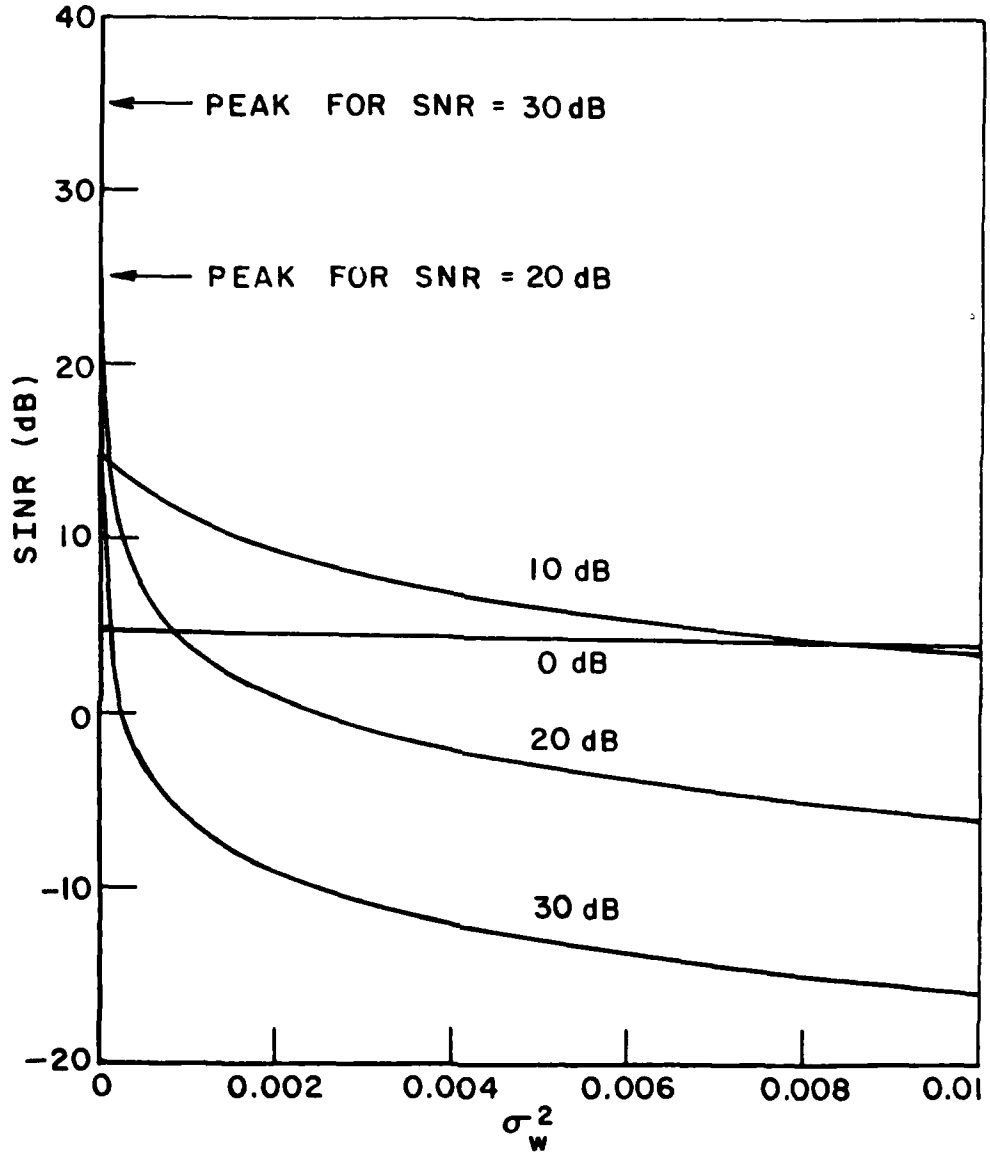

Figure 5. SINR vs σ_w^2

No interference, 3 elements, $\theta_d = 0^o$, $B_d = 0$

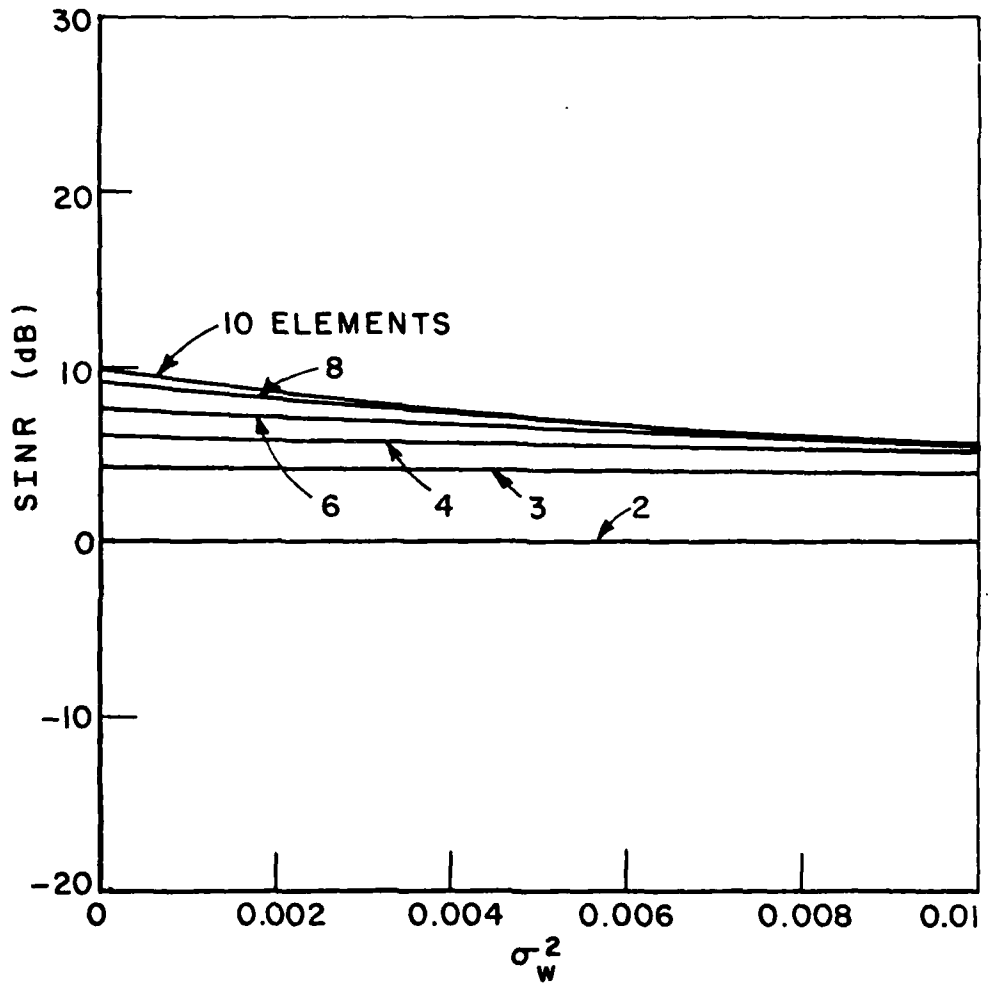

Figure 6. SINR vs σ_w^2

$\theta_d = 0^0$, $B_d = 0$, SNR = 0 dB

$\theta_i = 30^0$, $B_i = 0$, INR = 40 dB

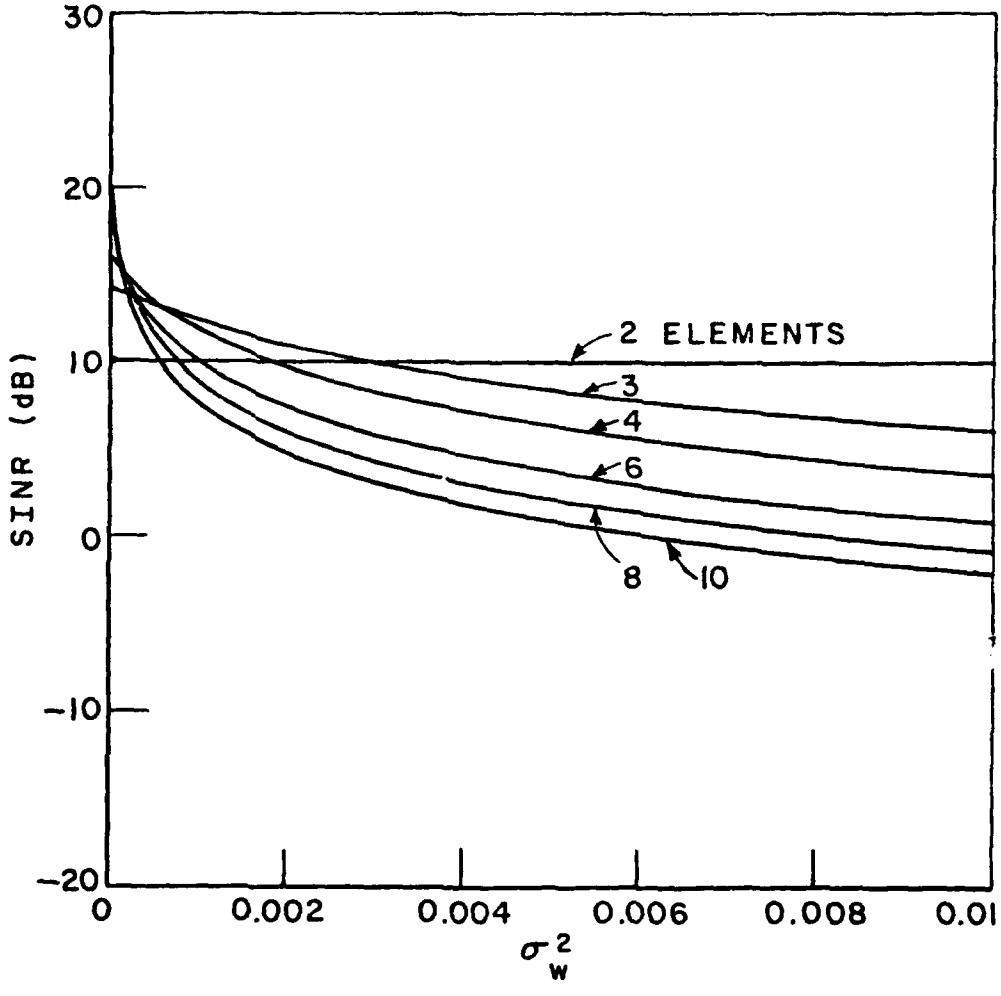

Figure 7. SINR vs σ_w^2

$\theta_d = 0^o$, $B_d = 0$, SNR = 10 dB
$\theta_i = 30^o$, $B_i = 0$, INR = 40 dB

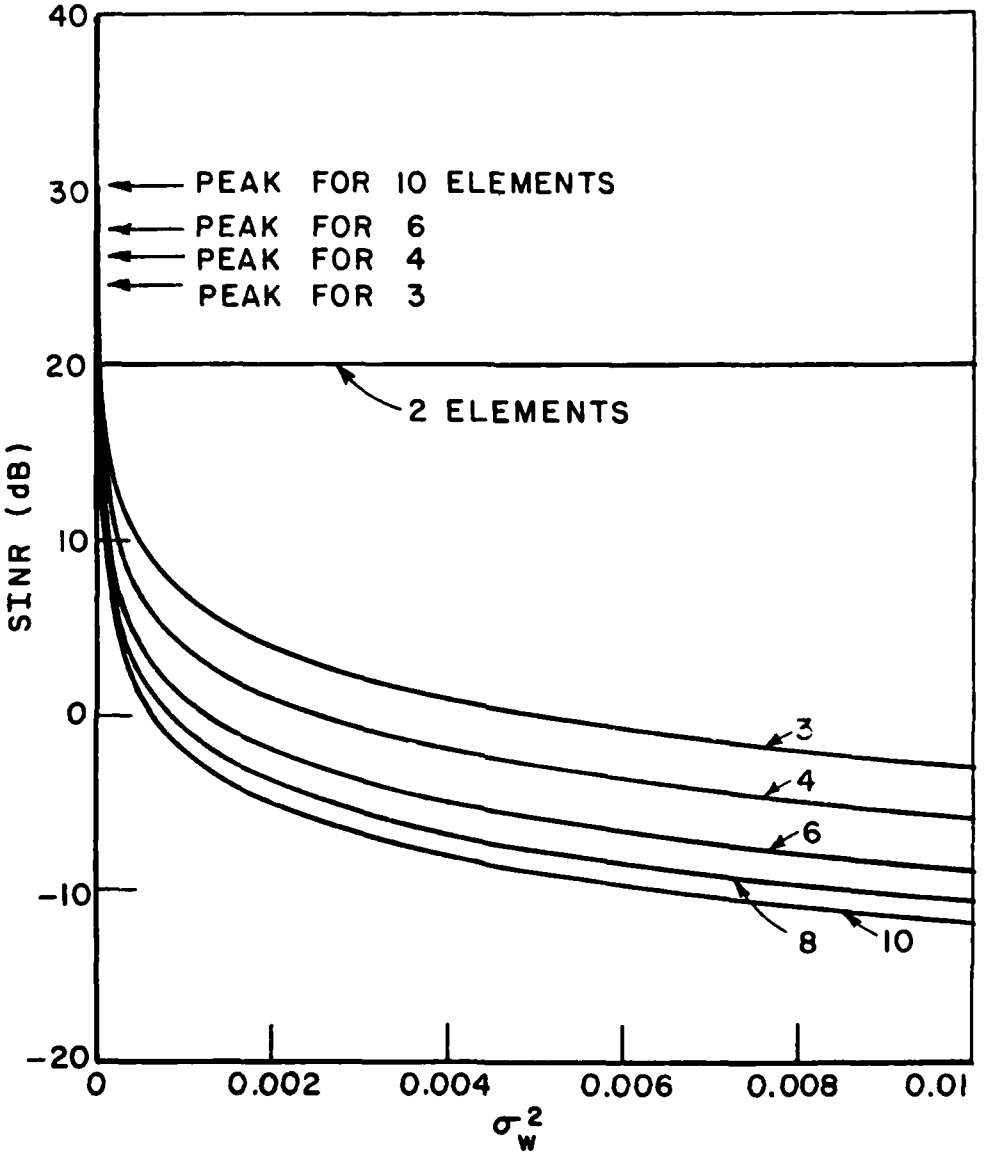

Figure 8. SINR vs σ_w^2

$\theta_d = 0^o$, $B_d = 0$, SNR = 20 dB

$\theta_j = 30^o$, $B_j = 0$, INR = 40 dB

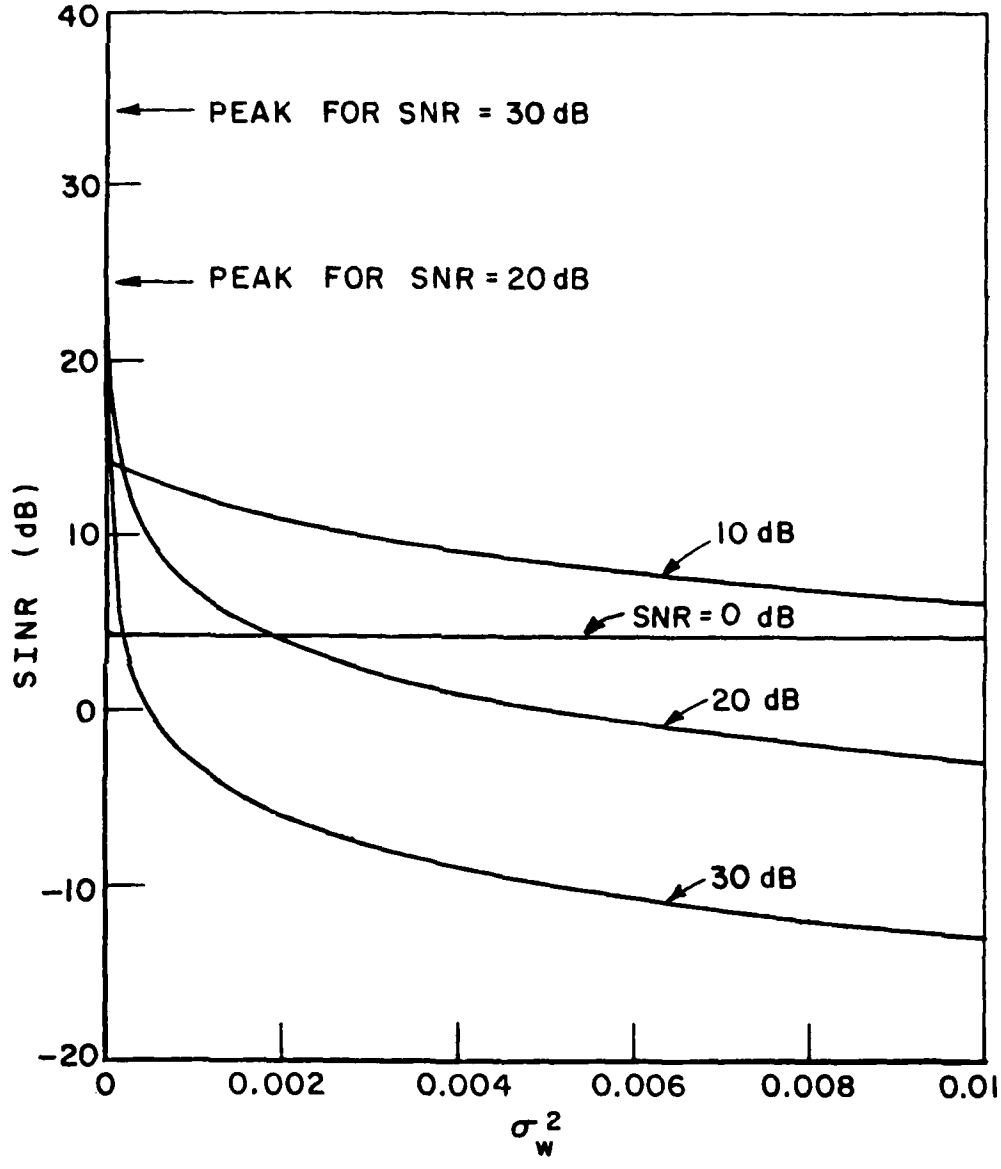

Figure 9. SINR vs. σ_w^2

3 elements, $\theta_d = 0^o$, $B_d = 0$

$\theta_i = 30^o$, $B_i = 0$, INR = 40 dB

elements to the array, one must hold σ_w^2 below a certain bound. As the SNR increases, this bound decreases.

Third, Figures 2-4 show that the sensitivity of the SINR to σ_w^2 increases as the SNR increases. For ξ_d = 0 dB, Figure 2 shows that the drop in SINR with σ_w^2 is small. But for ξ_d = 10 dB (Figure 3) the SINR drops more quickly with σ_w^2, and for ξ_d = 20 dB (Figure 4), the drop is even more rapid. For a fixed number of elements, the effect of SNR may be seen by plotting the SINR versus σ_w^2 with the SNR as a parameter. Figure 5 shows such a plot for a 3-element array and for SNR = 0, 10, 20, and 30 dB. It is again seen how increasing the SNR increases the sensitivity of the SINR to σ_w^2.

Next, we add an interference signal to the problem. Figures 6-9 show calculations similar to those in Figures 2-5 except that now an interference signal is present at $\theta_i = 30^0$ with an INR of 40 dB and zero bandwidth B_i. Figure 6 shows SINR versus σ_w^2 for ξ_d = 0 dB and for 2, 3, 4, 6, 8, and 10 elements. Figure 7 shows similar results for ξ_d = 10 dB, and Figure 8 shows ξ_d = 20 dB. Figure 9 shows the SINR versus σ_w^2 for a 3-element array for several SNRs.

Comparing the curves in Figures 6-9 with those in Figures 2-5 shows that the interference has a small influence on the sensitivity of the SINR to σ_w^2. The SINR drops slightly more quickly as a function of σ_w^2 without interference than with it. This result occurs because the interference null "uses up" one degree of freedom in the pattern. With interference present, there is less flexibility left in the pattern

to null the desired signal.*

A different perspective on these results may be gained by plotting the SINR as a function of the SNR with σ_w^2 as a parameter. Figure 10 shows such a plot, for the case of 3 elements and no interference. This type of curve shows that the error variance σ_w^2 that can be tolerated basically depends on the desired signal dynamic range that must be accommodated by the array. For a given σ_w^2, the SINR at first rises with SNR and then drops. The larger σ_w^2, the smaller the range of SNR over which the SINR remains high. If $\sigma_w^2 = 10^{-6}$, for example, the SINR exceeds 10 dB for 5 dB $\leq$ SNR $\leq$ 44 dB. But if $\sigma_w^2 = 10^{-4}$, the SINR exceeds 10 dB only for 5 dB $\leq$ SNR $\leq$ 24 dB. Each order of magnitude increase in σ_w^2 decreases the available desired signal dynamic range by 10 dB.

The bandwidth of the desired signal, B_d, has no effect on the results in Figure 10, because the desired signal arrives from $\theta_d = 0$. At this angle, the interelement time delay is zero, so there is no decorrelation of the signals in different array elements. However, if the desired signal arrives off broadside, B_d affects the performance. It turns out that bandwidth has the most effect when $B_d = 90^0$, because this case gives the most decorrelation between element signals.

---

*For the special case of a 2-element array, there is only one degree of freedom in the pattern to begin with. Hence, when an interference signal is present, there is no further flexibility in the pattern, other than its overall absolute magnitude, regardless of the particular error components δ_k. Since a change in pattern magnitude does not effect the SINR (it scales all signals proportionally), the SINR in Figures 6-8 does not depend on σ_w^2 for the case of 2 elements.

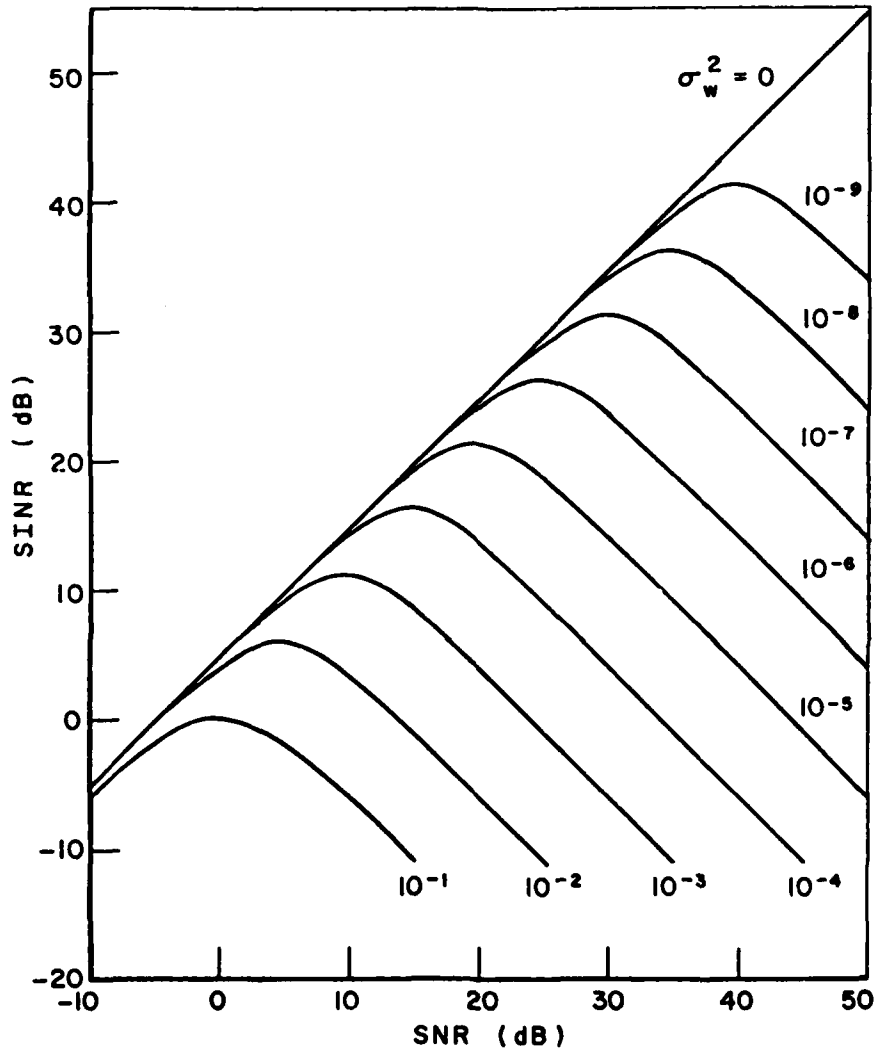

Figure 10. SINR vs SNR
No interference, 3 elements
$\theta_d = 0^o$, $0 \leq B_d \leq 0.5$

To illustrate the effect of bandwidth, we first assume there are no errors in the steering vector ($\sigma_w^2 = 0$). Under this condition, Figure 11 shows the SINR plotted versus the SNR for $\theta_d = 90^o$, for several values of B_d in the range $0 \leq B_d \leq .5$. It is seen that B_d causes a substantial degradation in array performance even for $\sigma_w^2 = 0$.

Now suppose $\sigma_w^2 \neq 0$. Figure 12 shows the SINR versus the SNR for several values of σ_w^2 and for B_d in the range $0 \leq B_d \leq .05$. In these curves, the bandwidth has a large effect only for $\sigma_w^2 \leq 10^{-6}$. For larger values of σ_w^2, the SINR has already been suppressed far enough by the steering vector errors that a nonzero bandwidth causes little additional degradation.

Finally, we consider the effect of an interference signal on these curves. Figure 13 shows typical curves of SINR versus SNR for $\theta_d = 0^o$, $\theta_i = 30^o$ and INR = 40 dB. Curves are shown for several values of interference bandwidth B_i in the range $0 \leq B_i \leq .1$. For lower values of SNR, where the steering vector errors are not affecting performance (for example, for the region SNR $\leq$ 20 dB if $\sigma_w^2 = 10^{-6}$), increasing B_i reduces the SINR in the well-known manner [2, 6]. (For $B_i \neq 0$ the interference is not nulled as well so the SINR is reduced.) For higher values of SNR, however, where steering vector errors degrade performance, increasing B_i actually <u>increases</u> the SINR. This curious behavior occurs because, as B_i becomes larger, the array must use more degrees of freedom to null the interference, so there are fewer left to null the desired signal. With a 3-element array (as in Figure 13), for example, there are 2 degrees of freedom. If $B_i = 0$, the array can null the interference

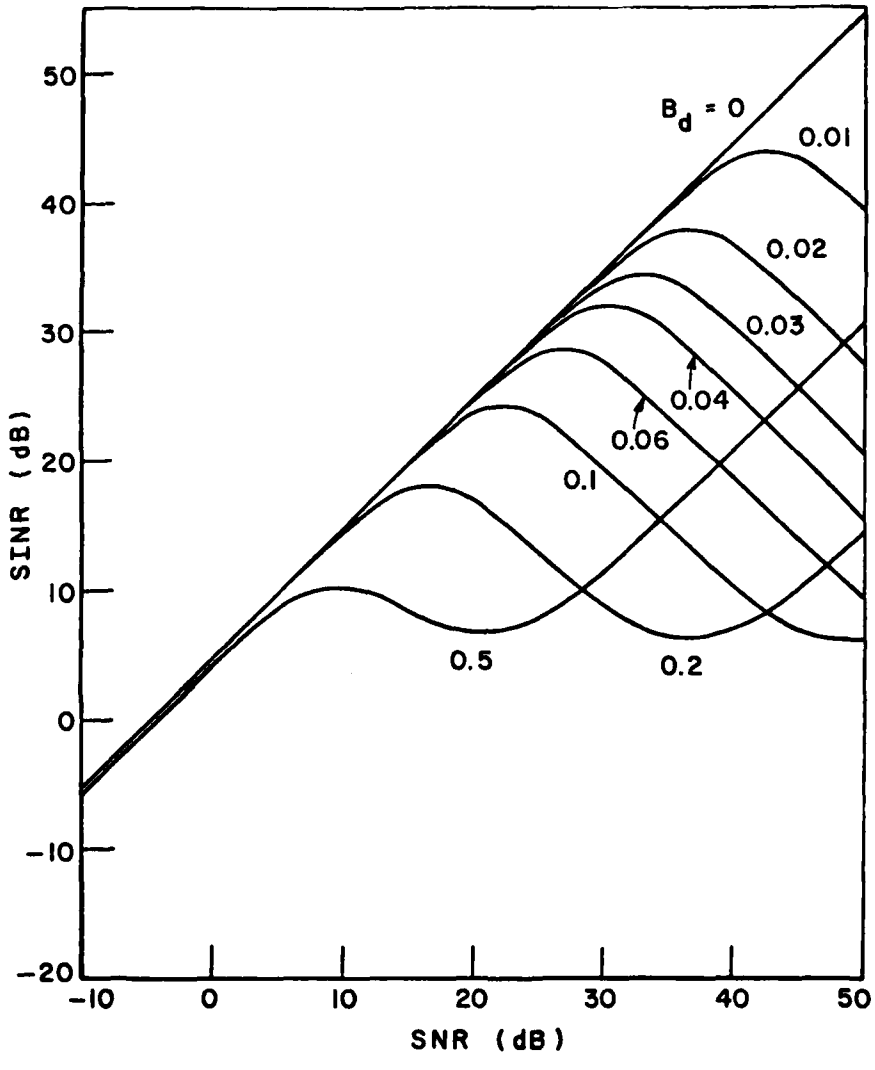

Figure 11. SINR vs SNR
No interference, 3 elements
$\theta_d = 90^0$, $\sigma_w^2 = 0$

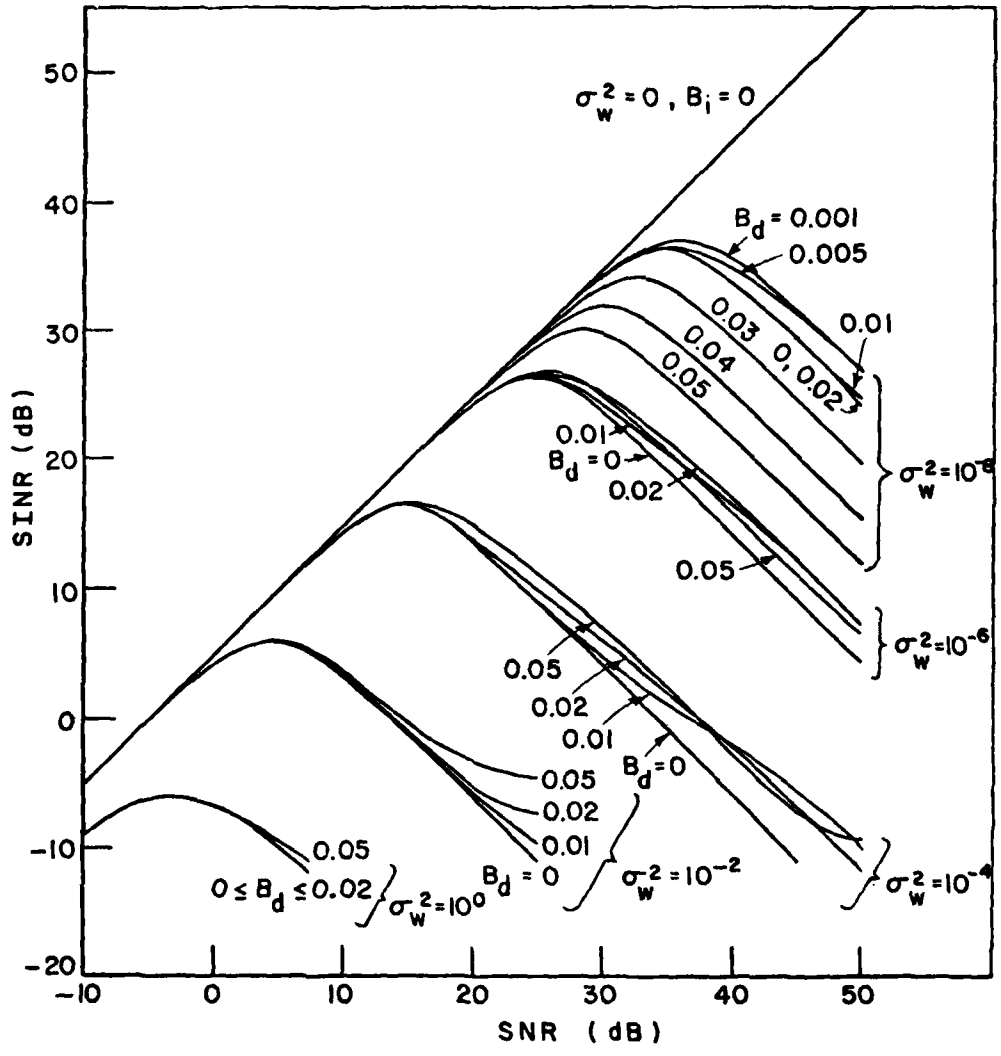

Figure 12. SINR vs SNR

No interference, 3 elements

$\theta_d = 90^0$

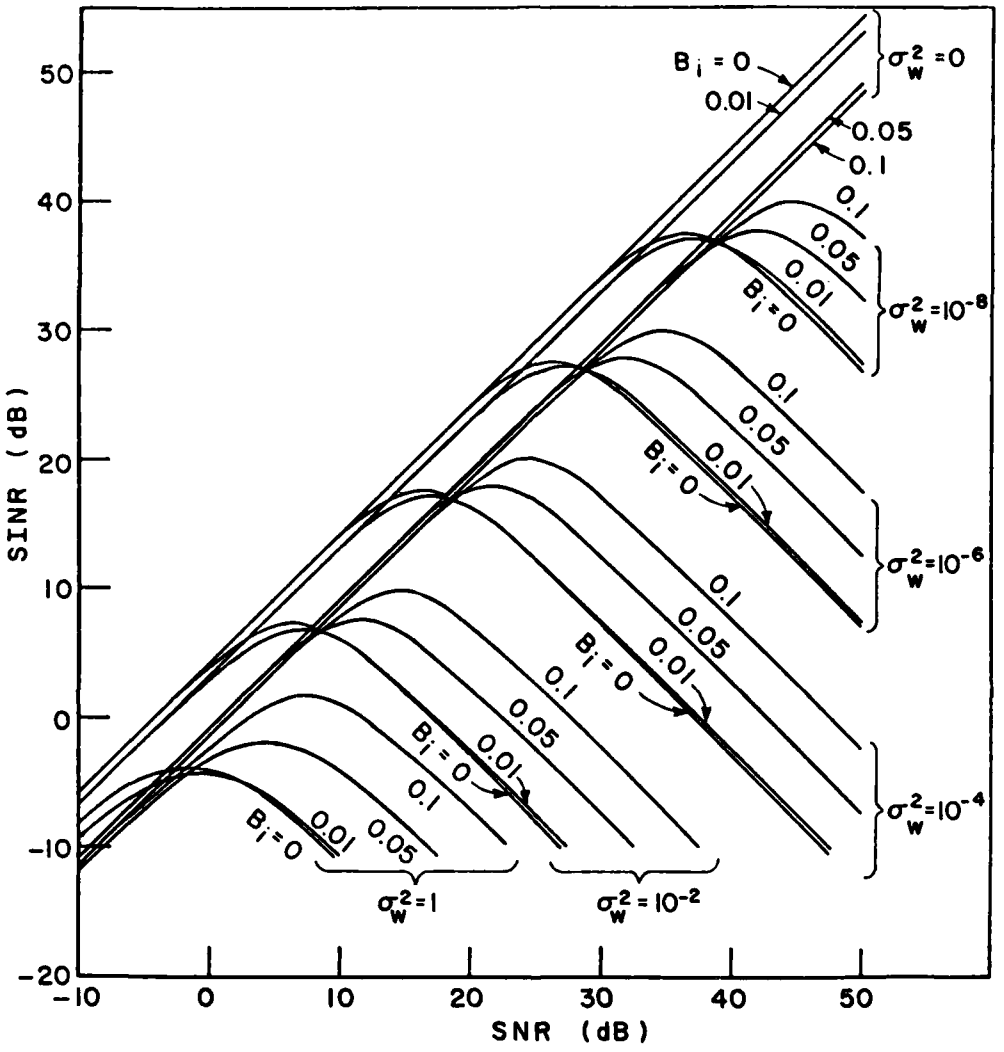

Figure 13. SINR vs. SNR
3 elements, $\theta_d = 0^0$, $0 \leq B_d \leq 0.1$
$\theta_i = 30^0$, INR = 40 dB

with one degree of freedom and then use the other one to reduce the desired signal. But, when B_i is increased, the array must use both degrees of freedom to obtain adequate interference nulling. (It does this by providing 2 nulls in the frequency band occupied by the interference.) The result is that there are no degrees of freedom left to null the desired signal. Hence, the output desired signal power is suppressed less than if $B_i = 0$ and the SINR remains higher. Studies of the array patterns as σ_w^2 and B_i are varied confirm this behavior.

IV. CONCLUSIONS

In this paper we have examined the effect of random steering vector errors on the performance of an Applebaum array. We assumed each component of the steering vector contained a random error with variance σ_w^2. The errors were assumed uncorrelated from one element to another.

It was shown that the array output SINR can drop quickly as a function of the error variance σ_w^2. The sensitivity of the output SINR to σ_w^2 is larger the higher the number of elements in the array and the larger the SNR. The presence of an interference signal has only a small effect on the sensitivity of the SINR to σ_w^2. The value of σ_w^2 that may be tolerated for a given application depends on the desired signal dynamic range that must be accomodated. The larger the dynamic range, the smaller σ_w^2 must be.

REFERENCES

1. S.P. Applebaum, "Adaptive Arrays," IEEE Trans. Antennas Propagat., vol. AP-24, p. 585, Sept. 1976.
2. R.T. Compton, Jr., "Pointing Accuracy and Dynamic Range in a Steered Beam Adaptive Array," IEEE Trans. Aerospace and Electronic Systems, vol. AES-16, p. 280, May 1980.
3. B. Widrow, P.E. Mantey, L.J. Griffiths and B.B. Goode, "Adaptive Antenna Systems," Proc. IEEE, vol. 55, p. 2143, Dec. 1967.
4. R.L. Riegler and R.T. Compton, Jr., "An Adaptive Array for Interference Rejection," Proc. IEEE, vol. 61, p. 748, June 1973.
5. I.S. Reed, J.D. Mallett, L.E. Brennan, "Rapid Convergence Rate in Adaptive Arrays," IEEE Trans. Aerospace and Electronic Systems, vol. AES-10, p. 853, November 1974.
6. R.T. Compton, Jr., "The Power Inversion Array - Concept and Performance," IEEE Trans. Aerospace and Electronic Systems, vol. AES-15, p. 803, Nov. 1979.


DATE
ILME